# Supporting Information

## Novel conducting solid polymer electrolytes with zwitterion structure boosting ionic conductivity and retarding lithium dendrite formation

Muhammad Irfan,[a] Yunlong Zhang,[a] Zeheng Yang,[a] Jianhui Su,[b,c] and Weixin Zhang*[a,b]

[a]*School of Chemistry and Chemical Engineering, and School of Materials Science & Engineering, Hefei University of Technology, Hefei, Anhui, 230009, PR China*

[b]*Institute of Energy, Hefei Comprehensive National Science Center, Hefei, Anhui, 230031, PR China*

[c]*School of Electrical Engineering and Automation, Hefei University of Technology, Hefei, Anhui, 230009, PR China*

**Corresponding author. Email: wxzhang@hfut.edu.cn (W. X. Zhang)*

## Experimental details

### Materials

1,8- diaminonaphthalene (DAN), 4,4′-diamino-3,3′-dimethyl diphenylmethane (DDPM), diethylether, 1,8 diaminooctane (DAO), glycidyltrimethylammonium chloride, N,N-dimethylformamide (DMF), and sulfosuccinic acid were bought from Aladdin Industrial Corporation (Shanghai, China). Lithium ferrous phosphate, N-Methyl-2-pyrrolidone, tetraethoxysilane, N,N-Dimethylacetamide (DMAc), acetylene black and lithium bis(trifluoromethanesulfonyl)imide were bought from Sinopharm Chemical Reagent Co., Ltd. These chemicals have analytical grade and were used during experiments.

### General characterization methods

The nuclear magnetic resonance (NMR) spectra of 1,8- diaminonaphthalene (DAN), 4,4′-diamino-3,3′-dimethyl diphenylmethane, 1,8 diaminooctane (DAO), quaternized DAN (Q-DAN), glycidyltrimethylammonium chloride (GTAC), quaternized DMP (Q-DMP), and quaternized DAO (Q-DAO) were received through a Agilent UNMRS600 US NMR instrument at 300 MHz. The morphological study of CSPEs was carried out by field emission scanning electron microscopy (FESEM, Hitachi SU8020). For SEM analysis, a clean membrane was cut into several pieces while it was frozen and broke in liquid nitrogen to prepare samples for cross-sectional morphology. Atomic force microscopy (AFM) images were recorded using a dimension icon microscope (Burker, Germany). The energy dispersive spectroscopy (EDS) confirmed the elemental compositions of PFPO and DN-PF-LCP CSPE. XPS analysis was carried out on Thermo ESCALAB250Xi instrument. The DN-PFPO-LCP, DMP-PFPO-LCP, and DAO-PFPO-LCP CSPEs and PFPO compositions were examined through peak areas investigation after standardization. The XPS peaks, mapping, and EDS spectra have been examined for the confirmation of quaternization, functionalization, and the availability of different functional groups in synthesized CSPEs. FT-IR spectra were obtained with a resolution of 2 $cm^{-1}$ using Nicolet 6700 (Thermo Fisher, USA) Spectrometer. Mechanical stability was evaluated at 25 $^{o}C$ using a Q 800 dynamic mechanical analyzer (DMA, TA Instruments, USA) with a stretching rate of 0.5 N $min^{-1}$. The thermogravimetric analysis was carried out under the nitrogen flow for the DN-PF-LCP, DMP-PF-LCP, and DAO-PF-LCP CSPEs by TGA 8000 analyzer, USA within a temperature range of 30 $^{o}C$ to 800 $^{o}C$ and keeping the heating rate constant at 10 $^{o}C$ /min. Differential scanning calorimetry (DSC, Q2000, USA) of CSPEs was analyzed at a heating rate of 10 ℃/min under a nitrogen atmosphere with a temperature range from -80℃ to 200 ℃. The crystal structure of the as-prepared CSPEs was analyzed using X-ray diffraction (XRD, Rigaku, Rint-2000) with Cu-Ka radiation (k = 0.154178 nm) source.

## Synthesis of Q-DAN

Quaternized DAN (Q-DAN) was synthesized according to our previous study.[1] The synthetic process can be briefly described as 1,5-diaminonaphthalene (1.5 g, 9.4816 mmol) and glycidyltrimethylammonium chloride (2.875 g, 18.957 mmol) were reacted to produce Q-DAN (Fig. S1a). The solid black product was obtained during the synthetic process with 77 % yield (3.36 g) and examined through $^{1}H$ NMR as shown in Fig. S3e. $^{1}H$ NMR (d-DMSO, 400 MHz): δ 7.24 (d, J = 8.3 Hz, 2H), 7.05 (t, J = 7.8 Hz, 2H), 6.64 (d, J = 7.3 Hz, 2H), 5.50 (s, 4H), 4.02 (m, 2H), 3.51 (m, 4H), 3.39 (m, 18H), 2.85 (m, 2H), 2.62 (m, 2H).

## Synthesis of Q-DMP

Quaternized DDPM (Q-DMP) was synthesized by following the reaction of Fig. S1b. 1.5 g of 4,4′-diamino-3,3′-dimethyl diphenylmethane (DMP) (6.6277 mmol) was dissolved in 60 mL of N,N-dimethylformamide in a round bottom flask. After complete dissolution, 2.01 g of glycidyltrimethylammonium chloride (13.2554 mmol) was added to the solution and underwent reflux at 90 $^{o}$C for overnight. Then reacting mixture was washed with diethylether several times and dried in an oven at 60 $^{o}$C. A yellow viscous product with 71% yield (2.49 g) was obtained and the resultant product was analyzed by proton NMR (Fig. S3e). $^{1}$H NMR (d-DMSO, 600 MHz) δ 6.78 (dt, *J* = 21.5, 9.9 Hz, 2H), 6.65 (m, 4H), 6.47 (m, 4H), 5.98 (m, 2H), 4.78 (m, 2H), 4.32 (d, *J* = 55.1 Hz, 2H), 3.98 (m, 2H), 3.52 (m, 22H), 1.97 (m, 6H).

**Synthesis of Q-DAO**

Quaternized 1,8 diaminooctane (Q-DAO) was synthesized according to the reaction (Fig. S1c). 1.5 g of 1, 8 diaminooctane (DAO) (10.398 mmol) was dissolved in the 60 mL N, N dimethylformamide and underwent the dissolution. Then, 3.153 g of glycidyltrimethylammonium chloride (20.796 mmol) was added to the solution and the resultant mixture was refluxed at 90 $^{o}$C for 24 hours. Afterward, the resulting mixture underwent purification with diethylether as well as dried in an oven at 60 $^{o}$C. A dark brown product with 81% yield (3.769 g) was received as a final product and examined by $^{1}$H NMR as shown in Fig. S3g. $^{1}$H NMR (d-DMSO, 600 MHz) δ 8.26 (s, 2H), 7.94 (m, 2H), 4.07 (m, 4H), 3.58 (m, 12H), 3.31 (m, 4H), 2.96 (m, 4H), 2.68 (m, 2H), 1.19 (s, 18H).

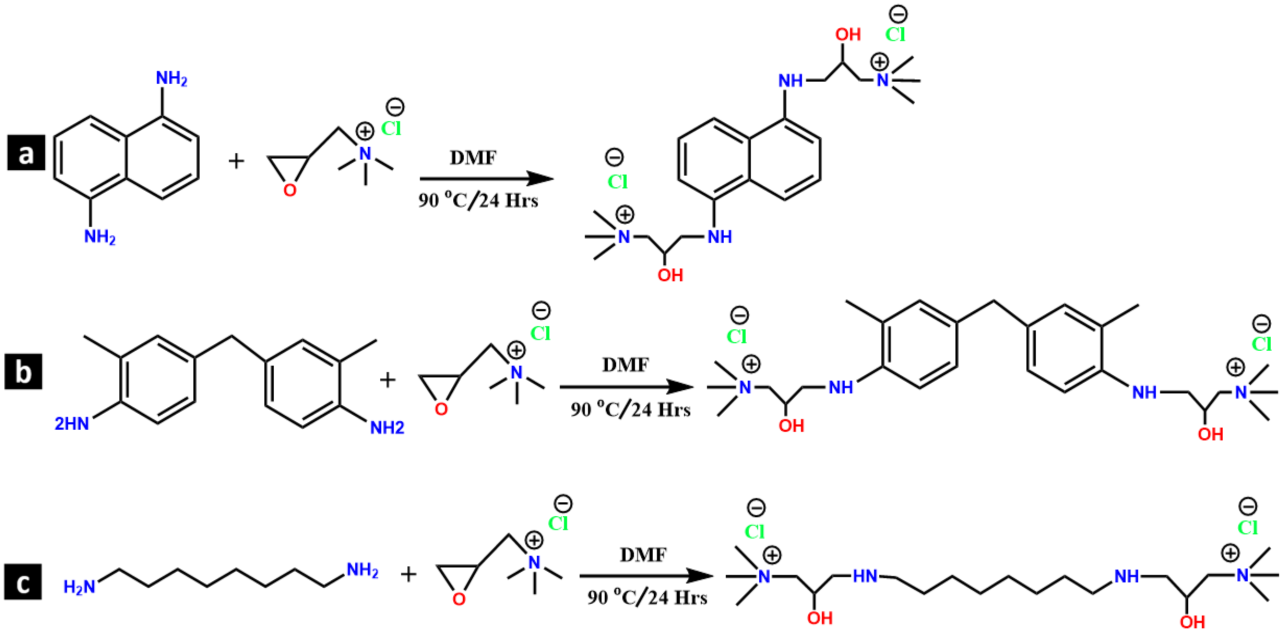

**Fig. S1** Synthesis of (a) Q-DAN, (b) Q-DMP, and (c) Q-DAO.

## Preparation of conducting solid polymer electrolytes

To a DMF solution of polyvinylidene fluoride (6 %) was added synthesized Q-DAN, Q-DMP, Q-DAO, sulfosuccinic acid, lithium bis(trifluoromethanesulfonyl)imide, tetraethoxysilane , and poly (ethylene oxide) according to Table S1. The synthesized Q-DAN, Q-DMP and Q-DAO were added in a specific molar ratio in the prescribed reaction mixture. The molar amount of SSA was kept greater than the other reactants (Table S1) to have an excess amount of carboxyl group for further functionalization. The reaction mixture was stirred at 60 °C for overnight. Then, the ionic polymer solution was cast on a glass plate and underwent drying in a vacuum oven for 24 h at 70 °C. After solvent evaporation, conducting solid polymer electrolyte (CSPE) was peeled off from the glass plate, and was placed in 0.01 M lithium hydroxide solution for 2 h and washed with DMAc and DMF, subsequently. Afterward, the CSPE was dried in a vacuum at 80 °C and then punched with 16 mm of diameter for electrochemical analysis. Based on the synthesized Q-DAN, Q-DMP and Q-DAO (Fig. S1), we have designed and fabricated a series of six CSPEs considering the effect of the polymeric backbone (PVDF, and PEO) simultaneously and donated by DN-PF-LCP, DN-PFPO-LCP, DMP-PF-LCP, DMP-PFPO-LCP, DAO-PF-LCP, and DAO-PFPO-LCP (Fig. S2). The dry CSPEs were obtained with a thickness of 195-210 µm. The thickness of the as-prepared CSPEs were controlled on clean glass plates using the casting blade during the casting process.

**Table S1** Compositions of the series CSPEs during preparation.

| CSPEs | PVDF (g) | PEO (g) | Q-DAN mmol | Q-DMP mmol | Q-DAO mmol | SSA mmol | LiTFSI mmol | TEOS mmol |
|---|---|---|---|---|---|---|---|---|
| DN-PF-LCP | 0.70 | - | 0.65 | - | - | 0.86 | 0.35 | 0.09 |
| DN-PFPO-LCP | 0.70 | 0.05 | 0.65 | - | - | 0.86 | 0.35 | 0.09 |
| DMP-PF-LCP | 0.70 | - | - | 0.65 | - | 0.86 | 0.35 | 0.09 |
| DMP-PFPO-LCP | 0.70 | 0.05 | - | 0.65 | - | 0.86 | 0.35 | 0.09 |
| DAO-PF-LCP | 0.70 | - | - | - | 0.65 | 0.86 | 0.35 | 0.09 |
| DAO-PFPO-LCP | 0.70 | 0.05 | - | - | 0.65 | 0.86 | 0.35 | 0.09 |

**Solid cathode preparation**

The $LiFePO_4$ electrode was synthesized via mixing the $LiFePO_4$, acetylene black (ACB), and poly(vinylidene fluoride (HSV900 PVDF) with a mass ratio of 8:1:1 in N-methylpyrrolidone (NMP). The mixture was stirred for 24 h to form a uniform slurry and cast on an aluminum foil and placed in 60 $^{o}$C vacuum oven for receiving a stable electrode weight. Afterward, the coated aluminum foil was cut into several pieces with 12 mm diameter, and then shifted to the Ar filled glove box for further usage.

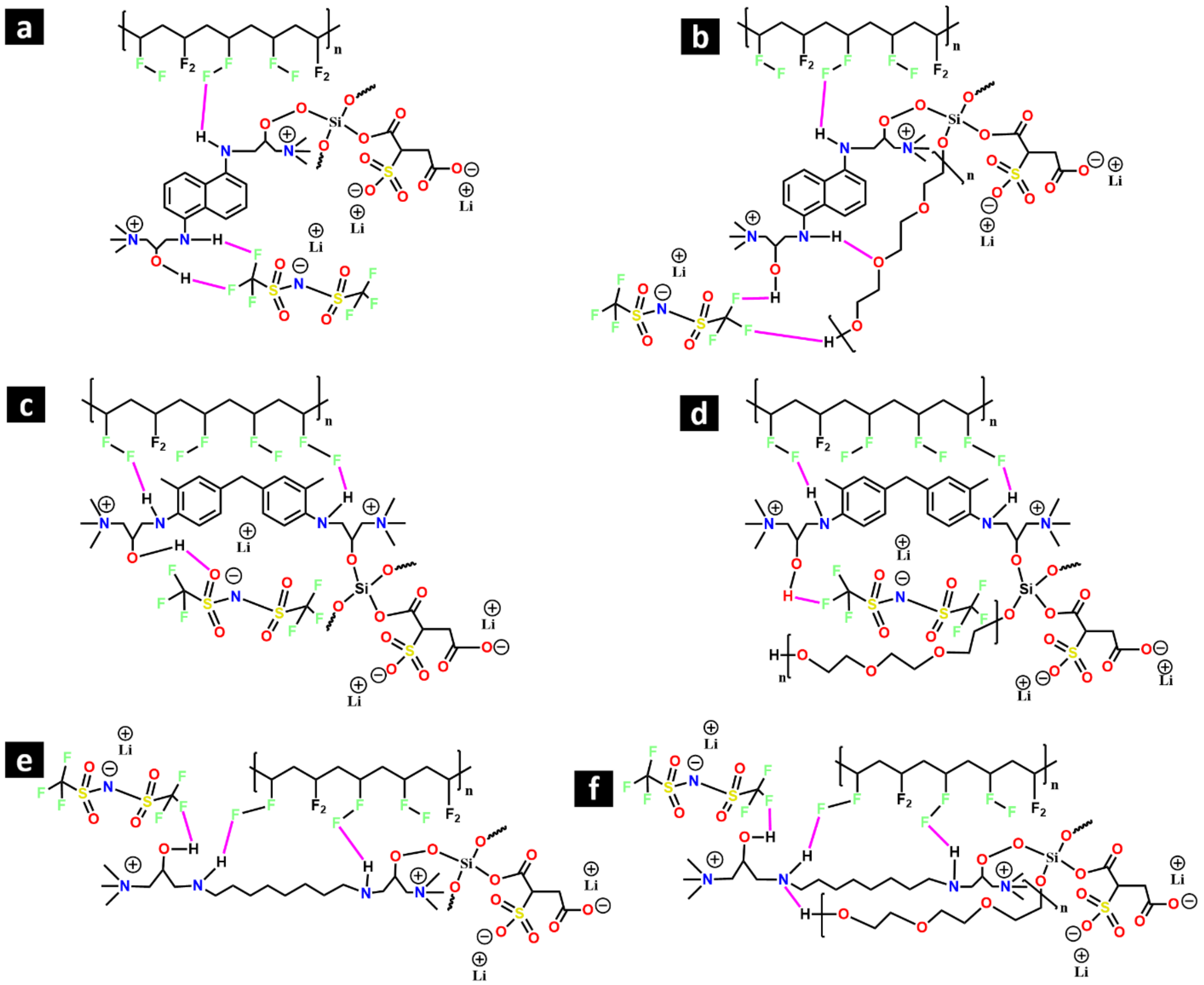

**Fig. S2** Synthesis of (a) DN-PF-LCP, (b) DN-PFPO-LCP, (c) DMP-PF-LCP (d) DMP-PFPO-LCP, (e) DAO-PF-LCP, and (e) DAO-PFPO-LCP CSPEs.

## Electrochemical characteristics

The ionic conductivity for the synthesized CSPEs was investigated by AC impedance spectroscopy analysis in a frequency range of 0.1-10$^6$ Hz. The cell was made as-synthesized CSPEs were sandwiched between stainless steel electrodes via SS | film | SS configuration. The measurement of ionic conductivity for the equipped cell was performed at 25 $^{o}$C. Ionic conductivity ($\sigma$) was determined by using the following equation (1).

$$\sigma = \frac{l}{RA} \qquad (1)$$

where l is the thickness of CSPE in cm, R is resistance in Ω, and A is the CSPE area in ($cm^2$).

The lithium transference number (LTN) was investigated using the 'Li | film | Li' asymmetric cell in a glove box at 25 °C by adopting the AC impedance and DC polarization techniques. The cell underwent polarization by DC voltage of 10 mV for 4000 s to examine the initial and final current. The LTN is calculated from the combination of AC impedance and potentiostatic polarization by Eq (2) as proposed by Evans et al.[2]

$$LTN = \frac{I_s\,(\Delta V - I_o R_o)}{I_o(\Delta V - I_s R_s)} \qquad (2)$$

where ΔV is applied potential (10 mV) across the cell, $I_o$, $I_s$, $R_o$, and $R_s$ are the initial current, steady-state current, initial resistance, and steady-state resistance respectively.

The electrochemical window was examined on a LAND CT2001A testing system by '$LiFePO_4$ | film | Li' where the lithium foil acts as both the counter electrode and the reference electrode while the stainless steel serves as the working electrode. The cyclic voltammetry was measured with a potential range of 2.0 ~ 4.2 V (vs $Li^+$/Li). In the dry argon glove box, the coin batteries were assembled using the same configuration of cyclic voltammetry as"$LiFePO_4$ | film | Li" to examine the cycling performance, rate capability, and other electrochemical properties. The electrochemical stability window was obtained by using linear sweep voltammetry (LSV) conducted on the Li|CSPEs|SS batteries between 2.0 and 6.0 V vs. Li/$Li^+$ at a sweep rate of 10 mV/s.

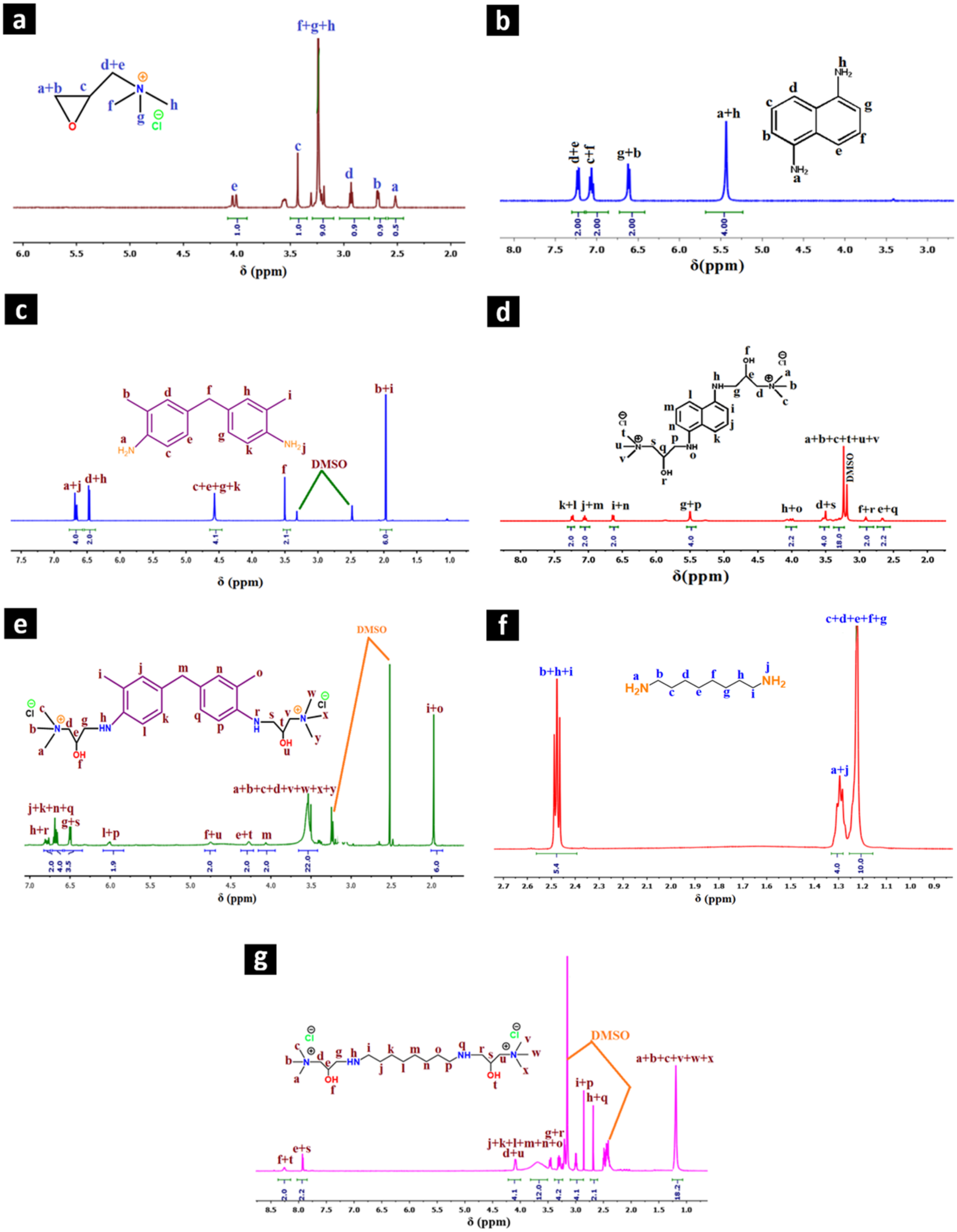

**Fig. S3** $^1$H NMR spectra of (a) GTAC (b) DAN (c) DMP (d) Q-DAN (e) Q-DMP (f) DAO and (g) Q-DAO.

## Results and Discussion

### Chronoamperometry analysis for synthesized CSPEs

The LTN may be also considered as an important parameter as the greater LTN efficiently reduced the concentration polarization that occurred via anions accumulation. The LTN values for the synthesized CSPEs are ranging from 0.67 to 0.40 (Fig. 4d). The addition of synthesized functional materials (i.e. Q-DAN, Q-DMP, Q-DAO), SSA, and TEOS act as favorable ion-dissociator to improve the LTN of prepared CSPEs due to hindering the movement of anions where the ionic current was predominantly carried out by $Li^+$ ions rather than its counter ions and enhanced the charging rates as well as the energy density of LIBs. Moreover, the $Li^+$ ions may interact with electron donor sites of CSPEs (N, and O atoms), thus weaken the polymeric backbone chain as well as enhance the amorphocity of the polymer host matrix to improve the electrical characteristics of fabricated CSPEs. Consequently, the migration of $Li^+$ ions becomes very fast due to the amorphousness of the polymer host matrix and promotes the LTN for CSPEs.

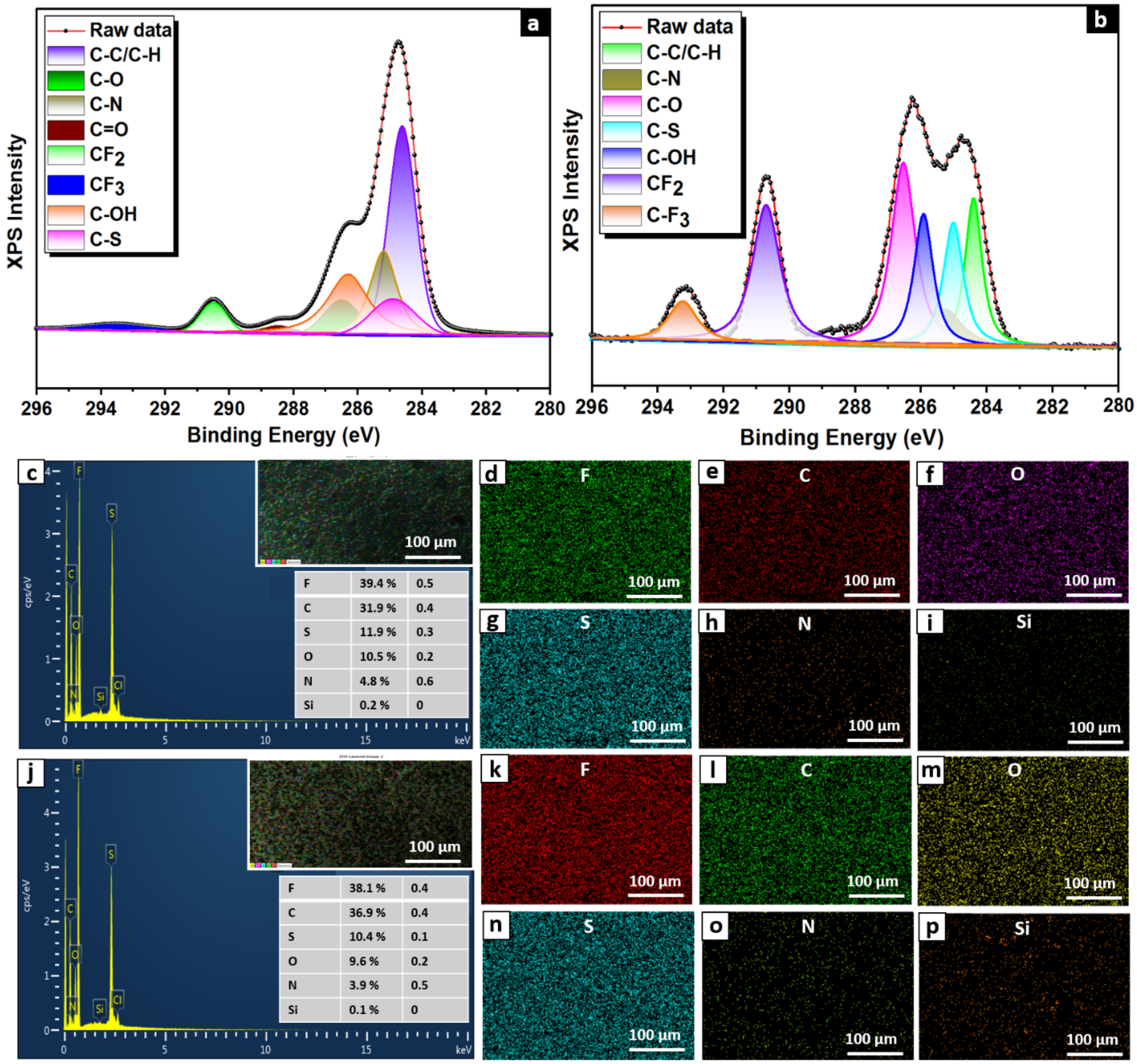

| | | |
|---|---|---|
| F | 39.4 % | 0.5 |
| C | 31.9 % | 0.4 |
| S | 11.9 % | 0.3 |
| O | 10.5 % | 0.2 |
| N | 4.8 % | 0.6 |
| Si | 0.2 % | 0 |

| | | |
|---|---|---|
| F | 38.1 % | 0.4 |
| C | 36.9 % | 0.4 |
| S | 10.4 % | 0.1 |
| O | 9.6 % | 0.2 |
| N | 3.9 % | 0.5 |
| Si | 0.1 % | 0 |

**Fig. S4** The high-resolution C1s of (a) DAO-PF-LCP and (b) DN-PFPO-LCP. EDS spectra of (c) DMP-PF-LCP, and (j) DAO-PF-LCP. (d-i) EDS mapping of F, C, O, S, N, and Si for DMP-PF-LCP, and (k-p) EDS mapping of F, C, O, S, N, and Si for DAO-PF-LCP.

**Table S2** The ionic conductivities of all-solid-state CSPEs in the previous decade.

| **SPEs** | **Ionic conductivity ( S cm$^{-1}$)** | **Temperature** | **Ref.** |
|---|---|---|---|
| Poly(PEGM)-b-poly(LiMTFSI) Copolymers | $2.3\times10^{-6}$ | 25 °C | [3] |
| LiX/PEO blended polymer electrolytes | $10^{-7}$ | 25 °C | [4] |
| CNF/PEO solid polymer electrolyte | $3.1\times10^{-5}$ | 25 °C | [5] |
| Silica-based polymer composite single-ion conductors | $10^{-6}$ | 80 °C | [6] |
| Si-PSSLi/PEGDME electrolytes | $3.16\times10^{-7}$ | 25 °C | [7] |
| PEO–PFSILi solid electrolytes | $1.78\times10^{-9}$ | 25 °C | [8] |
| PEO-PSLiTFSI electrolyte | $3.0\times10^{-8}$ | 25 °C | [9] |
| Li[PSTFSI-co-MPEGA] copolymer electrolytes | $7.6\times10^{-6}$ | 25 °C | [10] |
| Single-ion conductor triblock copolymer P(STFSILi)-*b*-PEO-*b*-P(STFSILi) | $1.3\times10^{-5}$ | 60 °C | [11] |
| SSPE-30 membrane | $1.42 \times 10^{-4}$ | 25 °C | [12] |
| Alternating diblock copolymer electrolytes | $6.61\times10^{-6}$ | 30 °C | [13] |
| PEO8−LiPCSI SPE | $8.32 \times 10^{-5}$ | 65 °C | [14] |
| LiPSTFSI+VIPS/PEO solid polymer electrolyte | $8.39 \times10^{-5}$ | 90 °C | [15] |
| LiPSS@PMMA SIPE | $0.97 \times 10^{-3}$ | 25 °C | [16] |

| | | | |
|---|---|---|---|
| SII-LE | $1.45 \times 10^{-4}$ | 25 $^{o}$C | [17] |
| s-CPEG electrolyte membrane | $1.84 \times 10^{-4}$ | 30 $^{o}$C | [18] |
| UiOLiTFSI | $2.07 \times 10^{-4}$ | 25 $^{o}$C | [19] |
| IPULi-1000 | $8.91 \times 10^{-7}$ | 30 $^{o}$C | [20] |
| LATP electrolyte | $1.58 \times 10^{-4}$ | 28 $^{o}$C | [21] |
| PISA-SPEs | $1.73 \times 10^{-4}$ | 26 $^{o}$C | [22] |
| MPyr-TFSI + Li-TFSI/PYR14-TFSI solid-state films | $1 \times 10^{-4}$ | 28 $^{o}$C | [23] |
| DN-PF-LCP | $8.69 \text{ x } 10^{-4}$ | 25 $^{o}$C | This work |
| DMP-PF-LCP | $6.46 \text{ x } 10^{-4}$ | 25 $^{o}$C | This work |
| DAO-PF-LCP | $4.69 \text{ x } 10^{-4}$ | 25 $^{o}$C | This work |
| DN-PFPO-LCP | $3.51 \text{ x } 10^{-4}$ | 25 $^{o}$C | This work |
| DMP-PFPO-LCP | $2.68 \text{ x } 10^{-4}$ | 25 $^{o}$C | This work |
| DAO-PFPO-LCP | $9.07 \text{ x } 10^{-5}$ | 25 $^{o}$C | This work |

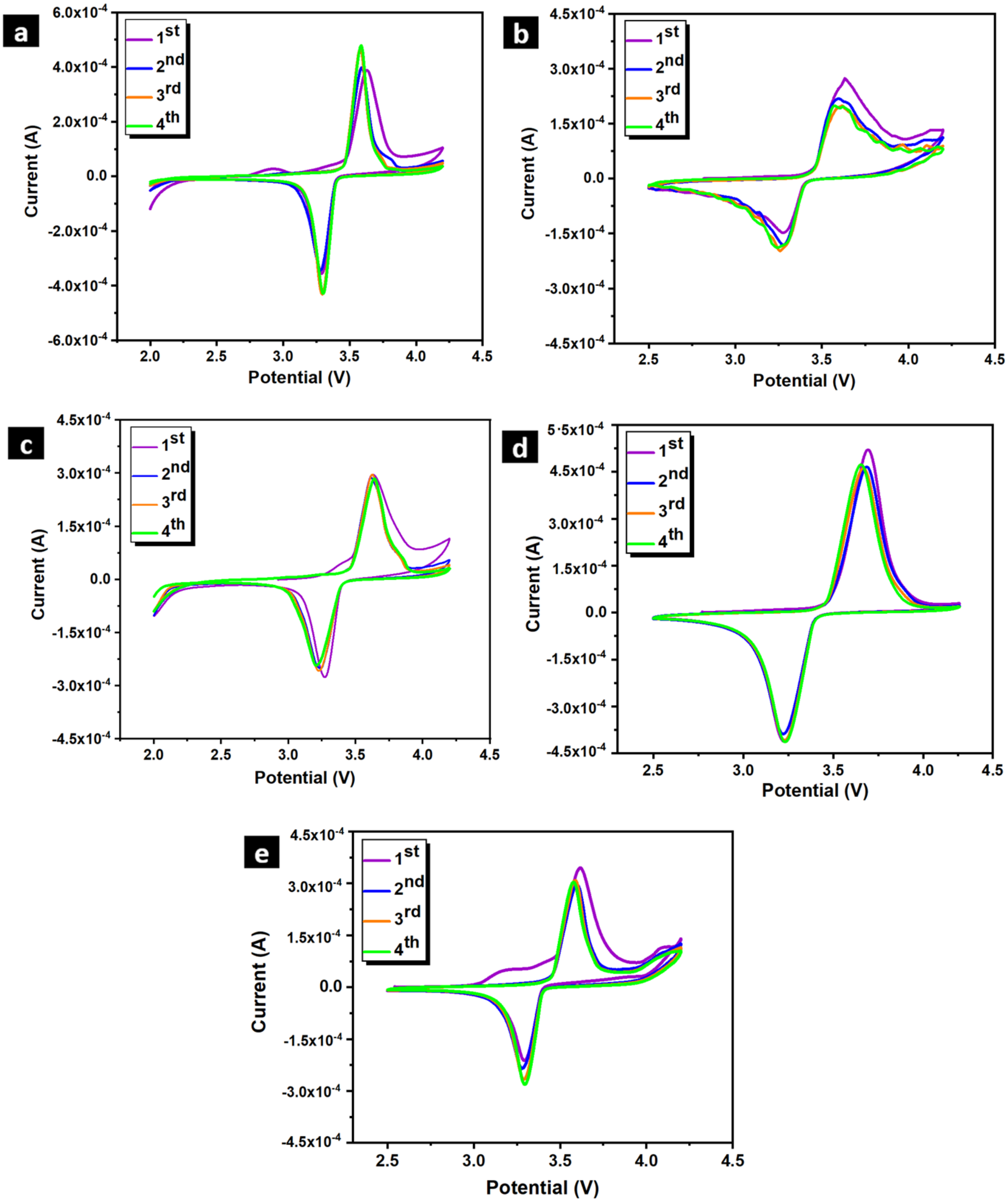

**Fig. S5** Cyclic voltammogram of $LiFePO_4$ electrode with CSPEs between +2.4 and +4.2 V (vs. $Li/Li^+$) at 25 $^oC$ and scan rate of 0.1 $mVs^{-1}$ for (a) DMP-PF-LCP (b) DAO-PF-LCP (c) DN-PFPO-LCP (d) DMP-PFPO-LCP, and (e) DAO-PFPO-LCP.

## References

1. M. Irfan, T. Xu, L. Ge, Y. Wang and T. Xu, *J. Membr. Sci.*, 2019, **588**, 117211.
2. J. Evans, C. A. Vincent and P. G. Bruce, *Polym.*, 1987, **28**, 2324-2328.
3. L. Porcarelli, A. S. Shaplov, M. Salsamendi, J. R. Nair, Y. S. Vygodskii, D. Mecerreyes and C. Gerbaldi, *ACS Appl. Mater. Interfaces*, 2016, **8**, 10350-10359.
4. Q. Ma, H. Zhang, C. Zhou, L. Zheng, P. Cheng, J. Nie, W. Feng, Y. S. Hu, H. Li, X. Huang, L. Chen, M. Armand and Z. Zhou, *Angew. Chem. Int. Ed.*, 2016, **55**, 2521-2525.
5. H. Qin, K. Fu, Y. Zhang, Y. Ye, M. Song, Y. Kuang, S. H. Jang, F. Jiang and L. Cui, *Energy Storage Mater.*, 2020, **28**, 293-299.
6. H. Zhao, F. Asfour, Y. Fu, Z. Jia, W. Yuan, Y. Bai, M. Ling, H. Hu, G. Baker and G. Liu, *ACS Appl. Mater. Interfaces*, 2015, **7**, 19494-19499.
7. H. Zhao, Z. Jia, W. Yuan, H. Hu, Y. Fu, G. L. Baker and G. Liu, *ACS Appl. Mater. Interfaces*, 2015, **7**, 19335-19341.
8. Q. Shi, L. Xue, D. Qin, B. Du, J. Wang and L. Chen, *J. Mater. Chem. A*, 2014, **2**, 15952-15957.
9. S. Inceoglu, A. A. Rojas, D. Devaux, X. C. Chen, G. M. Stone and N. P. Balsara, *ACS Macro Lett.*, 2014, **3**, 510-514.
10. S. Feng, D. Shi, F. Liu, L. Zheng, J. Nie, W. Feng, X. Huang, M. Armand and Z. Zhou, *Electrochim. Acta*, 2013, **93**, 254-263.
11. R. Bouchet, S. Maria, R. Meziane, A. Aboulaich, L. Lienafa, J. P. Bonnet, T. N. Phan, D. Bertin, D. Gigmes and D. Devaux, *Nat. Mater.*, 2013, **12**, 452-457.
12. C. Cao, Y. Li, S. Chen, C. Peng, Z. Li, L. Tang, Y. Feng and W. Feng, *ACS Appl. Mater. Interfaces*, 2019, **11**, 35683-35692.

13. Y. Chen, Y. Tian, Z. Li, N. Zhang, D. Zeng, G. Xu, Y. Zhang, Y. Sun, H. Ke and H. Cheng, *J. Membr. Sci.*, 2018, **566**, 181-189.

14. H. Yuan, J. Luan, Z. Yang, J. Zhang, Y. Wu, Z. Lu and H. Liu, *ACS Appl. Mater. Interfaces*, 2020, **12**, 7249-7256.

15. F. Lu, G. Li, Y. Yu, X. Gao, L. Zheng and Z. Chen, *Chem. Eng. J.*, 2020, **384**, 123237.

16. G. Chen, C. Niu, Y. Chen, W. Shang, Y. Qu, Z. Du, L. Zhao, X. Liao, J. Du and Y. Chen, *Solid State Ion.*, 2019, **341**, 115048.

17. K. L. Liu, C. H. Chao, H. C. Lee, C. S. Tsao, J. Fang, N. L. Wu and C. Y. Chao, *J. Power Sources*, 2019, **419**, 58-64.

18. Y. Zhao, Y. Bai, A. Liu, W. Li, M. An, Y. Bai and G. Chen, *J. Power Sources*, 2020, **450**, 227614.

19. F. Zhu, H. Bao, X. Wu, Y. Tao, C. Qin, Z. Su and Z. Kang, *ACS Appl. Mater. Interfaces*, 2019, **11**, 43206-43213.

20. Y. Fei, S. Liu, Y. Long, L. Lu, Y. He, X. Ma and Y. Deng, *Electrochim. Acta*, 2019, **299**, 902-913.

21. J. Zhang, S. Wang, D. Han, M. Xiao, L. Sun and Y. Meng, *Energy Storage Mater.*, 2020, **24**, 579-587.

22. B. Yuan, G. Luo, J. Liang, F. Cheng, W. Zhang and J. Chen, *J. Energy Chem.*, 2019, **38**, 55-59.

23. T. L. Chen, R. Sun, C. Willis, B. F. Morgan, F. L. Beyer and Y. A. Elabd, *Polym.*, 2019, **161**, 128-138.